New Phytologist

# A permineralized Early Cretaceous lycopsid from China and the evolution of crown clubmosses

Fabiany Herrera[1] (iD), Weston L. Testo[2,3] (iD), Ashley R. Field[4,5] (iD), Elizabeth G. Clark[6] (iD), Patrick S. Herendeen[7] (iD), Peter R. Crane[8,9] (iD) and Gongle Shi[10] (iD)

[1]Earth Sciences, Negaunee Integrative Research Center, Field Museum of Natural History, Chicago, IL 60605, USA; [2]Department of Biological and Environmental Sciences, University of Gothenburg, Gothenburg 405 30, Sweden; [3]Gothenburg Global Biodiversity Centre, Box 461, Gothenburg 405 30, Sweden; [4]Queensland Herbarium, Department of Environment and Science, Mount Coot-tha Botanic Gardens, Brisbane, Qld 4870, Australia; [5]Australian Tropical Herbarium, James Cook University, Cairns, Qld 4878, Australia; [6]Department of Biology, Duke University, Durham, NC 27708, USA; [7]Chicago Botanic Garden, Glencoe, IL 60022, USA; [8]Yale School of Environment, Yale University, New Haven, CT 06511, USA; [9]Oak Spring Garden Foundation, Upperville, VA 20184, USA; [10]State Key Laboratory of Palaeobiology and Stratigraphy, Nanjing Institute of Geology and Palaeontology and Center for Excellence in Life and Paleoenvironment, Chinese Academy of Sciences, Nanjing 210008, China

## Summary

• Lycopodiaceae are one of three surviving families of lycopsids, a lineage of vascular plants with a fossil history dating to at least the Early Devonian or perhaps the Late Silurian (*c.* 415 Ma). Many fossils have been linked to crown Lycopodiaceae, but the lack of well-preserved material has hindered definitive recognition of this group in the paleobotanical record.

• New, exceptionally well-preserved permineralized lycopsid fossils from the Early Cretaceous (125.6 ± 1.0 Ma) of Inner Mongolia, China, were examined in detail using acetate peel and micro-computed tomography techniques. The anatomy of extant Lycopodiaceae was analyzed for comparison using fluorescence microscopy. Phylogenetic relationships of the new fossil to extant Lycopodiaceae were evaluated using parsimony and maximum likelihood analyses.

• *Lycopodicaulis oellgaardii* gen. et sp. nov. provides the earliest unequivocal and best-documented evidence of crown Lycopodiaceae and Lycopodioideae, based on anatomically-preserved fossil material.

• Recognition of *Lycopodicaulis* in Asia during the Early Cretaceous indicates the presence of crown Lycopodiaceae at this time, and striking similarities of stem anatomy with extant species provide a framework for the understanding of the interaction of branching and vascular anatomy in crown-group lycopsids.

## Introduction

Lycopsids, comprising the homosporous Lycopodiales and the heterosporous Selaginellales and Isoetales, are the only surviving members of a lineage of vascular plants with an evolutionary history of > 400 Myr (e.g. Thomas, 1992, 1997; Kenrick & Crane, 1997; Bateman *et al.*, 2007; Taylor *et al.*, 2009; Cleal & Thomas, 2019). As the sister group to all other vascular plants, lycopsids are also of exceptional interest for understanding land plant evolution and development (Spencer *et al.*, 2021). However, while the fossil record of heterosporous lycopsids is extensive and intensively studied based on well-preserved macrofossils and also megaspores, the evidence of the homosporous lineage is much more poorly understood.

Lycopodiaceae (clubmosses), the sole extant family of Lycopodiales, includes three subfamilies, 16 genera, and *c.* 400 species, all of which are homosporous, herbaceous, and have microphylls that lack ligules (Field *et al.*, 2016; PPG I, 2016; Testo *et al.*, 2018a). Most of the extant species of clubmoss belong to the subfamily Huperzioideae (i.e. *Huperzia* (*c.* 30 spp.), *Phlegmariurus* (*c.* 270 spp.), *Phylloglossum* (1 sp.)) which exhibit the most diversity of life forms in the family, including terrestrial, semi-aquatic, and epiphytic species (Øllgaard, 1992; Field *et al.*, 2016; Bauret *et al.*, 2018; Testo *et al.*, 2018b). The two remaining subfamilies, Lycopodielloideae (i.e. *Lateristachys* (*c.* 4 spp.), *Lycopodiella* (*c.* 15 spp.), *Palhinhaea* (*c.* 25 spp.), *Pseudolycopodiella* (*c.* 10 spp.)) and Lycopodioideae (i.e. *Austrolycopodium* (*c.* 8 spp.), *Dendrolycopodium* (*c.* 4 spp.), *Diphasiastrum* (*c.* 20 spp.), *Diphasium* (*c.* 5 spp.), *Lycopodiastrum* (1 sp.), *Lycopodium* (*c.* 15 spp.), *Pseudodiphasium* (1 sp.), *Pseudolycopodium* (1 sp.), *Spinulum* (*c.* 3 spp.)) include species that range in habit from semi-aquatics to robust scrambling, and clump-forming terrestrials (Field *et al.*, 2016). Molecular dating analyses estimate that crown-group Lycopodiaceae (i.e. a living monophyletic group or clade

consisting of the last common ancestor of all living species, plus all of its descendants including fossil taxa) likely originated during the Late Devonian, but most extant species evolved during the Cenozoic (e.g. Wikström & Kenrick, 2001; Bauret *et al.*, 2018; Testo *et al.*, 2018a). However, these analyses lack securely identified fossils for calibrating nodes within the family.

Despite the extensive record of Paleozoic and Mesozoic lycopsids, it has been challenging to recognize definitive fossils of crown-group Lycopodiaceae (see Skog & Hill, 1992; Thomas, 1992; Bateman *et al.*, 2007; Thomas, 2017), largely due to a lack of fossils with anatomy preserved, the difficulties of confirming the absence of ligules and therefore distinguishing vegetative remains from the distal twigs of species of Lepidodendrales, (Taylor *et al.*, 2009). A potential early lycopsid is *Asteroxylon mackiei* Kidston & Lang, an intricate early land plant from the 407-million-year-old Rhynie chert with unvascularized microphylls and a primitive actinostele (Kidston & Lang, 1920, 1921; Taylor *et al.*, 2009; Kerp *et al.*, 2013; Hetherington *et al.*, 2021). Another interesting Paleozoic plant, *Hestia eremosa* R.M. Bateman, Kenrick et Rothwell, from the Mississippian of Scotland (Bateman *et al.*, 2007) is based on fragmentary permineralized axes that are putatively herbaceous and eligulate with a stellate stele. During the early Mesozoic, lycopodialean fossils include isophyllous and anisophyllous species that resemble those of extant Lycopodiaceae (Skog & Hill, 1992; Thomas, 2017), but many of these species have been placed in *Lycopodites* Lindley & Hutton, a poorly understood genus for herbaceous shoots of possible clubmoss affinity. However, none of these occurrences can be assigned confidently to crown-group Lycopodiaceae.

This report presents new, superbly well-preserved permineralized vegetative axes from the Lower Cretaceous (125.6 ± 1.0 Ma) of Inner Mongolia, China, which provide the earliest and best-documented evidence of crown Lycopodiaceae. The morphology and anatomy of the fossil axes and microphylls allows secure placement in the Lycopodiaceae and provides a relationship to extant Lycopodioideae. The comprehensive anatomical review of extant lycopsids provides a framework for the future recognition of Lycopodiaceae fossils and the understanding of the branching and vascular anatomy in crown-group lycopsids.

## Materials and Methods

All fossils reported in this study were collected during fieldwork from 2017 to 2019 in the Zhahanaoer open-cast coal mine, Jarud Banner, eastern Inner Mongolia, China (location: 45°21′38.5″N, 119°25′04″E). The fossil material comes from massive but laterally restricted layers of chert in the Huolinhe Formation a sequence of fluvio-lacustrine and swamp deposits that vary from conglomerates, sandstones, siltstones and mudstones, intercalated with extensive coal layers in the Huolinhe Basin (Deng, 1995). The age of the chert at the Zhahanaoer locality has been determined as 125.6 ± 1.0 Ma (late Barremian–earliest Aptian) based on U–Pb zircon dating of crystals isolated from a volcanic ash that occurs just below the chert layers, and that is also consistent with associated palynological assemblages (G. Shi *et al.*, 2021; G. L. Shi *et al.*, 2021).

The fossils were revealed by physical sections of chert blocks made with a Hi-Tech Diamond 6″ trim saw (Fig. 1; Supporting Information Figs S1–S5). Anatomical details were obtained from acetate peels prepared after etching the polished slabs in 45% hydrofluoric acid for 50–60 s using the technique of Joy *et al.* (1956) and Galtier & Phillips (1999). Acetate peels were mounted on slides with Canada balsam, neutral balsam or Eukitt and then photographed with an Olympus BH-2 (BHTU) microscope at the Field Museum, Chicago, IL, USA, a Leica DMLB microscope fitted with a Progress Gryphax digital camera at the Chicago Botanic Garden, and a Leica M205A microscope and Leica DMC5400 digital camera system at the Nanjing Institute of Geology and Palaeontology, Chinese Academy of Sciences. Fossil material described in this study is housed in the paleobotanical collections of the Nanjing Institute of Geology and Palaeontology, Chinese Academy of Sciences with collection numbers designated with the prefix PB.

The morphology and anatomy of the fossils was also obtained by high-resolution computed tomography (CT) (Fig. 2) of key specimens using a GE dual tube X–ray scanner in the Department of Organismal Biology and Anatomy at the University of Chicago. The holotype was micro-CT imaged at beamline 8.3.2 of the Advanced Light Source at the Lawrence Berkeley National Laboratory (Berkeley, CA, USA). Then, 2159 two-dimensional images were generated with a voxel size of 0.65 μm. The digitized volume of the specimen was visualized using Avizo Lite 2020.2 (Thermo Fisher Scientific, Waltham, MA, USA). A volume thresholding tool in Avizo was used to digitally demarcate the three-dimensional (3D) volume of the digitized fossil specimen from the surrounding rock matrix. The digitized 3D volume was then extracted from the matrix as a wavefront (OBJ) file and imported into MESHLAB (Cignoni *et al.*, 2008). A screened Poisson surface reconstruction was applied in MESHLAB to estimate the shape of the external surface of the digitized volume (Kazhdan & Hoppe, 2013) following the semi-automated removal of polygons from the volume's interior. This representation of the external surface was exported as a watertight polygonal mesh and visualized and imaged using MAYA (Autodesk, San Rafael, CA, USA). CT data have been deposited in Figshare at https://figshare.com/s/e9959d343b8bfc95165e.

To compare the fossils to extant lycopsids, we examined 58 collections of fresh material and herbarium specimens (Figs 3, 4c, S6–S11; Table S1), representing 50 species belonging to 13 of the 16 recognized genera (PPG I, 2016). We also studied material of Selaginellaceae (1 sp.) and Isoetaceae (2 spp.) to compile a representative sample of the current global morphological, functional, and diversity of lycopsids. Anatomy was assessed following the procedure of Ayensu (1967) (see also Elpe *et al.*, 2018). Dried leafy stems were soaked and softened in a 6 : 1 mixture of aerosol–OT (10%, w/v) and acetone (95%, v/v) for at least 72 h, then stored in 70% ethanol in plastic vials. Stems from living material were treated in FAA (formalin, acetic acid, 70% (v/v) ethanol) for at least 7 d, then stored in 70% ethanol in plastic vials. Multiple transverse sections of erect, fertile and sterile stems and creeping shoots were obtained to assess anatomical variation of the cortex and stele along their axes. In a few cases roots and strobili were also
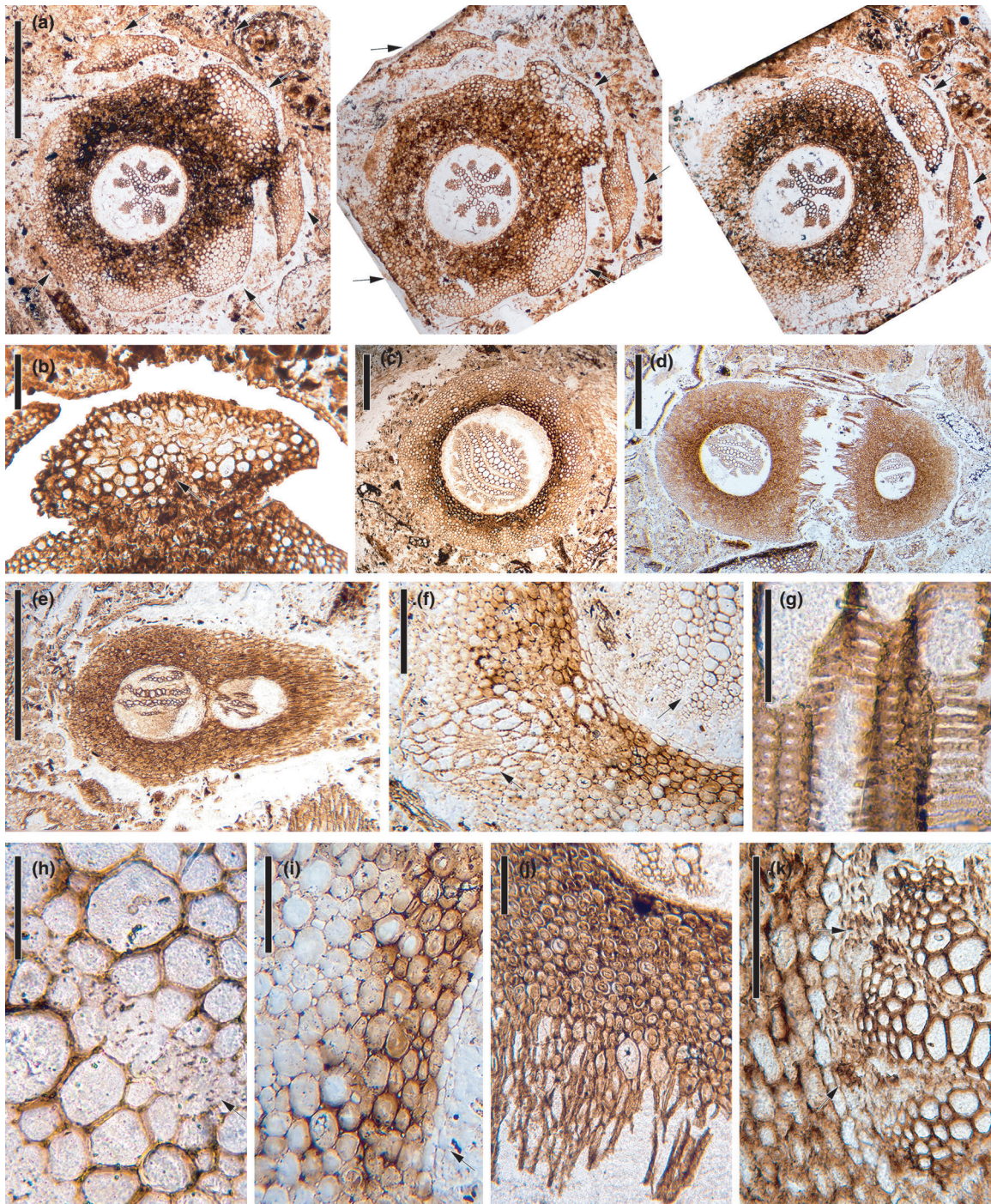
**Fig. 1** *Lycopodicaulis oellgaardii* gen. et sp. nov. light micrographs of acetate peels. (a) Holotype (PB23753), serial transverse sections (proximal to distal) of vegetative stem; note central actinostele and partially fused, then fully separated, microphylls (arrows). (b) Transverse section from holotype showing base of a microphyll close to the point of separation and vascular trace (arrow). (c) Axis with nearly circular transverse section showing actino–plectostele; note the light parenchymatous outer cortex and dark sclerenchymatous inner cortex (PB23762). (d, e) Axes showing dichotomous branching in transverse section and protosteles (PB23759, PB23751). (f) Detail of counterpart from (c) showing oblique transverse section of tracheids comprising the microphyll trace (left arrow) and narrow bands with probable sieve elements (right arrow) between the xylem arms of the actino–plectostele. (g) Detail of metaxylem tracheids in longitudinal section showing uniseriate slit-like scalariform pits (right) and circular bordered pits arranged in two rows (lower left) (PB23749). (h) Detail of part of actino–plectostele from (c); note two large metaxylem arms and narrow bands of poorly preserved phloem between (arrow). (i) Detail from (c) showing (right to left) pericycle-endodermis (arrow), sclerenchymatous inner cortex, and parenchymatous outer cortex. (j) Detail from (d) showing sclerenchymatous inner cortex at level of dichotomous branching; note few sclerenchyma cells in lateral view (bottom). (k) Detail of inner cortex and stele in transverse section showing three xylem arms with narrow bands of phloem in between (upper arrow); note at least four microphyll traces connected to protoxylem poles and pericycle-endodermis (one at lower arrow) (PB23758). Bars: (d) 1 mm; (a, c, e) 500 μm; (f) 200 μm; (b, i–k) 100 μm; (h) 50 μm; (g) 20 μm.
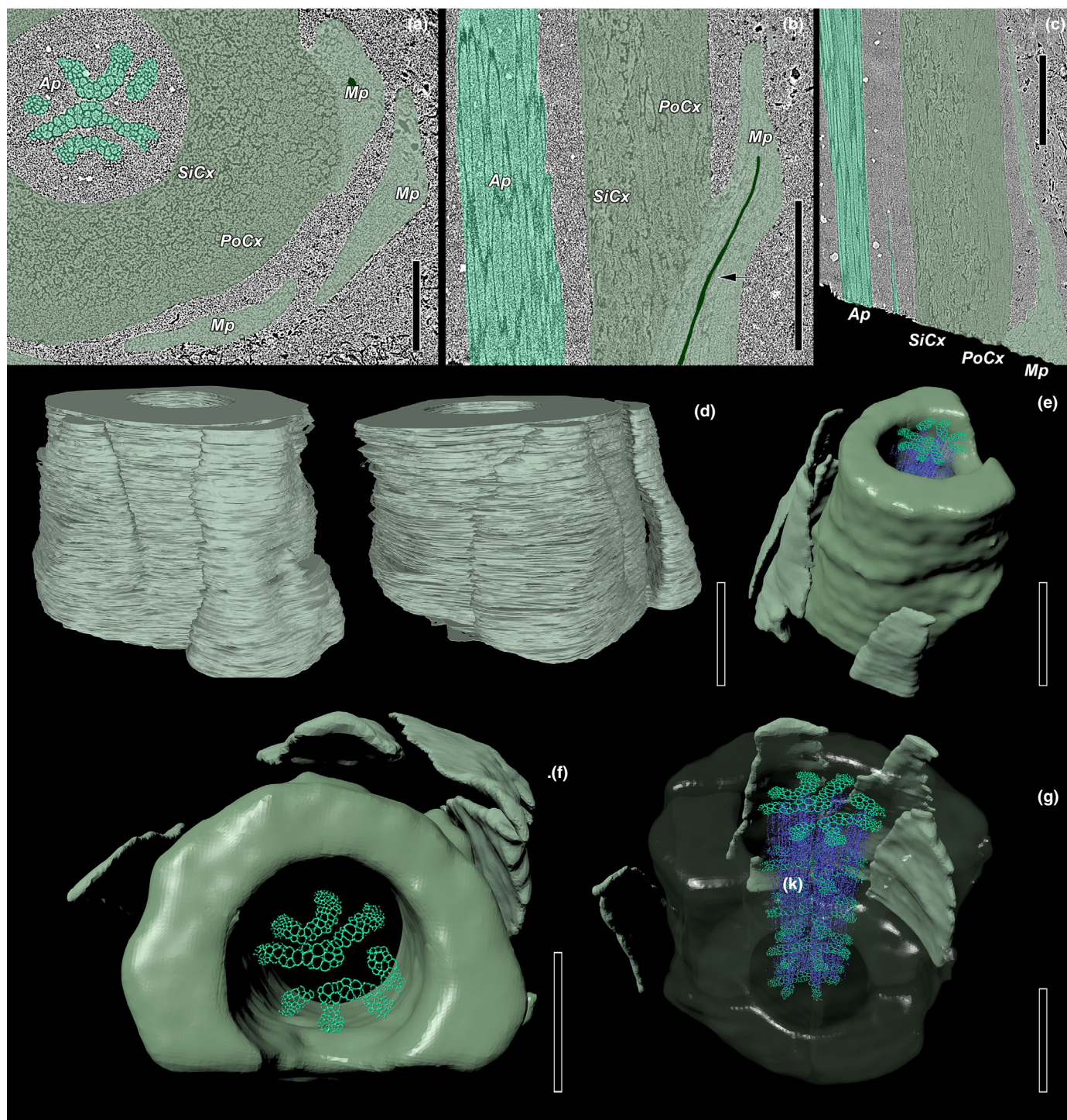
**Fig. 2** *Lycopodicaulis oellgaardii* gen. et sp. nov. (holotype, PB23753). Micro-computed tomography (micro-CT) images and three-dimensional reconstructions from segmented tomography data. (a) Transverse section of axis showing actinostelic protostele (*Ap*), sclerenchymatous inner cortex (*SiCx*), parenchymatous outer cortex (*PoCx*), and three microphylls (*Mp*). (b, c). Longitudinal sections showing actinostele with elongated tracheids, thick walled cells of the *SiCx*, and an attached *Mp*; note the course of the vascular trace extending into the *Mp* (arrow). (d) Lateral views of axis showing two attached microphylls; note slightly decurrent base. (e, f) Panoramic and vertical view of axis showing actinostele, cortex, and four microphylls. (g) Same reconstruction from (e) with semitransparent cortex showing the arrangement of actinostele at different levels. Bars: (e) 1 mm; (d, f, g) 500 μm; (a–c) 200 μm.

sectioned transversely (Figs S9, S10). Anatomical fresh sections were made with a hand microtome (Allmikro-Mikrotom, Nürnberg, Germany); the specimens were held between two pieces of polystyrene foam and then were secured inside the microtome device without the need to embed the axes. Fresh sections were immediately examined using fluorescence microscopy with a Leica

DMLB microscope (Lumen 200 Fluorescence Illumination System; Prior Scientific Inc., Rockland, MA, USA; filter set 02: G 365, FT 395, LP 420). Under autofluorescence xylem in the stele usually appears light blueish and the phloem bright pink, while autofluorescence of the cortex varied from light and dark blue to orange. Cuticle autofluoresced brightly from yellow, purple to white. Additional comparative data for extant Lycopodiaceae were obtained from available descriptions in the literature (e.g. Jones, 1905; Stokey, 1907; Hill, 1914; Pixley, 1968; Wilder, 1970; Chu, 1974; Warmbrodt & Evert, 1974a,b; Øllgaard, 1975, 1979, 1987, 1992, 2015; Bruce, 1976; Stevenson, 1976; Gola *et al.*, 2007; Carlquist *et al.*, 2012; Arana *et al.*, 2014; Rincón-Baron *et al.*, 2014; Lopes *et al.*, 2020).

To assess the relationships of the new fossil material to extant lycopsids, we developed a morphological matrix of 20 taxa and 26 morphological and anatomical characters (Table S2). The complete morphological matrix, including character definitions, states, and scorings is also available at the MorphoBank website (http://morphobank.org/permalink/?P3664). In addition to the new fossil material the matrix includes all genera of extant Lycopodiaceae, as well as *Isoetes* and *Selaginella*, and the fossil herbaceous lycopsid *Paurodendron stellatum* from the Permian of Antarctica (McLoughlin *et al.*, 2015).

Analyses were conducted on a combined morphological (all taxa) and DNA sequence (plastid *rbcL* and *psbA-trnH*; extant taxa) dataset. The combined matrix of 1540 characters is provided on MorphoBank web site as well. GenBank accession numbers for the DNA sequence data are provided in Table S3. The maximum likelihood (ML) topology (Fig. 4a) was inferred according to the best-fitting model based on the BIC criterion (MK+FQ+G4 model, BIC score = 26 306.6) using IQ-Tree web server (http://iqtree.cibiv.univie.ac.at/) (Trifinopoulos *et al.*, 2016). Statistical support for internal branches in the phylogeny was assessed by bootstrapping (1000 replicates). Maximum parsimony (MP) analyses (Fig. 4b) used *Isoetes* and *Selaginella* as the outgroups in heuristic searches with 10 000 replicates of random taxon addition and tree-bisection-reconnection (TBR) branch swapping in the program Paup* 4.0a (build 168) for Macintosh (X86) (Swofford, 2003). All morphological characters were treated as unordered and weighted equally. Bootstrap analyses were performed on the morphological data using 1000 replicates with full heuristic searches and heuristic searches with 10 random sequence additions.

## Results

### Systematics

Class – Lycopodiopsida
    Order – Lycopodiales
    Family – Lycopodiaceae
    Subfamily – Lycopodioideae
    Genus – *Lycopodicaulis* F. Herrera, Testo, A.R. Field, E. Clark, Herend., P.R. Crane et G. Shi gen. nov.
    Type – *Lycopodicaulis oellgaardii* F. Herrera, Testo, A.R. Field, E. Clark, Herend., P.R. Crane et G. Shi sp. nov.

Generic diagnosis – Vegetative axes unbranched to sparsely dichotomous and anisotomously (unequal) branched. Axes with a central to excentric protostele surrounded by a thin zone of endodermis/pericycle, a thick cortex, and a thin epidermis and cuticle. Protostele varying from actinostelic, actino-plectostelic to plectostelic, occupying more than one-third of the total stem diameter. Cortex consisting of an ill-defined inner sclerenchymatous layer and an ill-defined outer parenchymatous layer. Cortex lacking aerenchyma and emergent roots. Microphylls isophyllous, entire margined, glabrous, dorsiventrally flattened with an acute apex, and a slightly contracted and decurrent base. Microphylls lacking a ligule, with an entire margin, arranged spirally in six to eight ranks, widely spaced between alternating sub-whorls. Microphylls consisting of two layers of parenchyma and an unbranched vascular strand with no associated leaf gap. Leaf traces very small in transverse section in or near the vascular cylinder, but increasing in diameter in the cortex.

*Lycopodicaulis oellgaardii* F. Herrera, Testo, A.R. Field, E. Clark, Herend., P.R. Crane et G. Shi sp. nov.

Specific diagnosis – Actinostele arms with six to eight exarch protoxylem poles, actino–plectostelic to fully plectostelic steles with up to 14–18 exarch poles. Protoxylem consisting of three to seven files of tracheids; metaxylem consisting of 2–20 files of thick-walled tracheids. Walls of xylem tracheids with scalariform thickenings and circular borders on pits. Cortical cells in the sclerenchymatous layer strongly lignified. Microphylls elliptical, rhomboidal, to triangular in transverse sections. Cortical leaf traces with a distinctive parenchymatous bundle sheath.

Holotype – PB23753 (Figs 1a,b, 2, S1, S2).

Other specimens studied – PB23747–PB23752, PB23754–PB23766 (Figs 1c–k, S3–S5).

Repository – Paleobotanical Collections, Nanjing Institute of Geology and Palaeontology, Chinese Academy of Sciences (NIGPAS).

Locality – Zhahanaoer open-cast coal mine, Jarud Banner, eastern Inner Mongolia, China (location: 45°21′38.5″N, 119°25′04″E).

Stratigraphic position and age – Huolinhe Formation, late Barremian–earliest Aptian, 125.6 ± 1.0 Ma.

Etymology – 'lycopodi' referring to the Lycopodioideae affinity and the Latin 'caulis' for stem. The specific epithet in honor of Benjamin Øllgaard for his landmark contributions to the study of Lycopodiaceae.

Detailed description – Twenty diminutive permineralized vegetative axes were recovered from the Zhahanaoer chert (Figs 1, 2, S1–S5). The three dimensionally preserved axis fragments are 0.9–2.3 mm in diameter, and up to *c.* 4 mm long. Several axes showing the point of bifurcation (Figs 1d,e, S3a–c, S5) are 1.0–2.6 mm wide. Stems are unbranched to sparsely dichotomous–anisotomously branched (Figs 1c–e, 2, S3, S5a–g). Unbranched stems vary from elliptical to nearly circular in transverse section (e.g. Fig. 1a), but are broadly elliptical at or near branching points (e.g. Figs 1d,e, S5). Transverse sections and CT scans of the axes reveal a central to excentric protostele surrounded by a thin zone of endodermis/pericycle, a thick cortex, and a thin epidermis and cuticle (Figs 1, 2, S1, S3–S5).
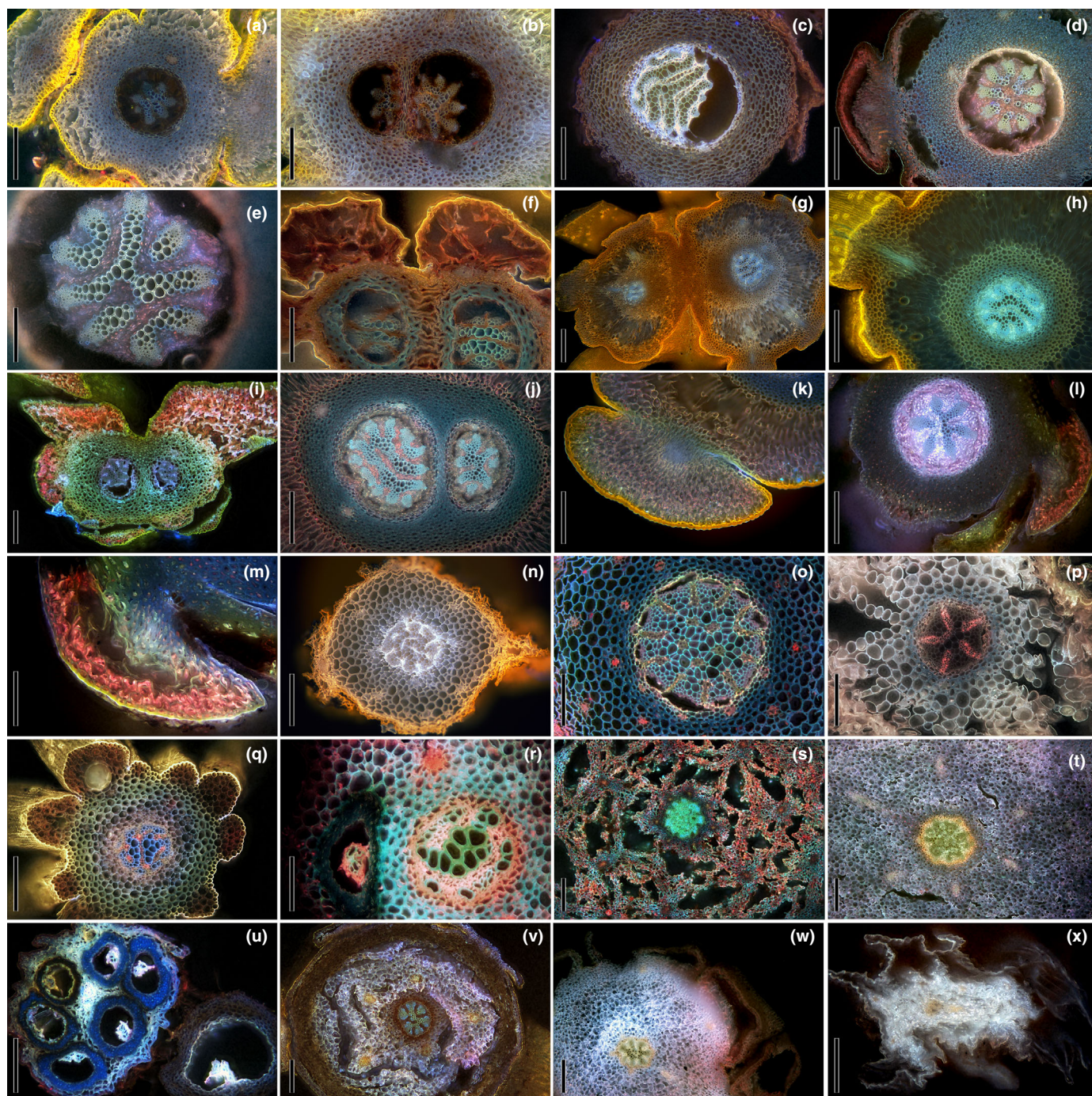
The actinostelic to plectostelic protostele occupies more than one-third of the total stem diameter and ranges from 0.2 to 1.2 mm in length in transverse section (Figs 1a,c–e, 2, S1, S3, S4d–g, S5). Actinosteles are usually in axes with diameters of < 1.0 mm and have six to eight exarch protoxylem poles (e.g. Figs 1a, S1, S3i), whereas plectosteles (e.g. Fig. 1d) and actino–plectosteles (e.g. Fig. 1c) are usually in axes with diameters of > 1.0 mm and have up to 14–18 exarch poles. The transition between the exarch protoxylem to the inner metaxylem is broadly defined by a change in the diameter of the tracheid lumens.

Protoxylem (Figs 1k, 2e–g, S1c,d, S4d–g) consists of three to seven files of tracheids that are mostly elliptical to circular in transverse section, and are $c.$ 2.5–7 µm in diameter and up to $c.$ 56–80 µm long. Metaxylem (Figs 1h,k, 2e–g, S1c,d, S4d–g) consists of approximately 2–20 files of thicker walled tracheids that vary from polygonal, circular, to elliptical in transverse section, and are $c.$ 8–57 µm in diameter and up to $c.$ 190–400 µm long. The largest metaxylem tracheids occur near the center of the axis (Figs 2b, S1c, S4a,b) and occasionally appear interspersed with tracheids of smaller diameter (as seen in transverse section). End-

**Fig. 3** Transverse sections of extant Lycopodiaceae under fluorescence microscopy (Lumen 200 Fluorescence Illumination System; filter set 02: G 365, FT 395, LP 420); representatives of the subfamilies Lycopodioideae (a–m), Lycopodielloideae (n–q), and Huperzioideae (r–x); terrestrial taxa (a–q, s, t, v, w), epiphytic (r, u), and semi-aquatic (x). (a–c) *Austrolycopodium magellanicum* (VT: Testo 1373, Colombia) erect leafy axis showing actino–plectostele and microphylls (a); dichotomous branching, note sclerenchymatous inner cortex (b); creeping axis showing plectostele (c). (d, e) *Spinulum annotinum* (VT: Testo 2473, USA) showing variation from actinostele (d) to actino–plectostele (e) along the same erect axis. (f) *Lycopodiastrum casuarinoides* (US: 1861795, Taam 2168, China) at level of dichotomous branching showing plectostele and sclerenchymatous inner cortex, note two microphylls. (g, h) *Lycopodium clavatum* (US: 3073425; Fleming 113, USA) at level of dichotomous branching showing plectostele, sclerenchymatous inner cortex, parenchymatous outer cortex, and several microphylls (g); detail of actino–plectostele, note leaf trace entering microphyll (h). (i) *Diphasium jussiaei* (VT: Testo 1728, Colombia) erect leafy axis at level of dichotomous branching. (j, k) *Diphasiastrum complanatum* (US: 3585123, Holt 639, Greenland) erect leafy axis at level of dichotomous branching showing conspicuous sclerenchymatous inner cortex and actino–plectostele (j); detail of microphyll showing leaf trace (k). (l, m) *Dendrolycopodium obscurum* (VT: Testo 2475, USA) erect leafy axis showing actino–plectostele and microphyll (l); detail of microphyll, note air spaces (m). (n) *Pseudolycopodiella caroliniana* (US: 3383165, Steury 990911.7, USA) showing actino–plectostele and parenchymatous cortex. (o) *Lycopodiella matthewsii* (VT: Testo 1323, Colombia) showing actino–plectostele and thin sclerenchymatous inner cortex, note leaf traces. (p) *Lycopodiella prostrata* (VT: Testo 1664, USA) showing actinostele and aerenchyma within parenchymatous cortex. (q) *Palhinhaea cernua* (US: 2259505, Tsang 28180, China) showing plectostele, parenchymatous inner cortex and sclerenchymatous outer cortex, note several microphylls. (r) *Phlegmariurus callitrichifolius* (VT: Testo 1186, Colombia) showing plectostele, parenchymatous cortex, and cortical emergent root (left). (s) *Phlegmariurus cocuyensis* (VT: Testo 1390, Colombia) showing small diameter of actino–plectostele and aerenchyma within parenchymatous cortex. (t) *Phlegmariurus rufescens* (VT: Testo 1744, Colombia) showing small diameter of actino–plectostele and parenchymatous cortex. (u) *Phlegmariurus linifolius* var. *planifolius* (VT: Testo 1318, Colombia) showing small diameter of actino–plectostele surrounded by six cortical emergent roots. (v) *Huperzia lucidula* (VT: Testo 2472, USA) showing small diameter of actino–plectostele, parenchymatous inner cortex with aerenchyma, note leaf traces. (w) *Huperzia continentalis* (US: 3501322, Sladen 21, USA) showing small diameter of actino–plectostele, parenchymatous cortex, and lacunae within microphyll. (x) *Phylloglossum drummondii* (US: 1371348, Brame, New Zealand) showing small diameter of plectostele, parenchymatous cortex, and lacunae within microphyll. Bars: (g, i, s, t, v, w) 500 µm; (a–d, h, j–l, n–q, u, x) 400 µm; (e, f, m, r) 200 µm.

walls of xylem tracheids are tapered (Figs 2b,c, S1b). Walls of xylem tracheids have mostly scalariform thickenings and occasional circular borders on pits that are mainly in the metaxylem (Fig. 1g). Scalariform thickenings are *c.* 8–9 µm wide and are separated by slit-like pits; circular bordered pits are *c.* 2.6–3.4 µm wide and are arranged in two rows. In most cases, the phloem is not preserved, except in a few specimens that show poorly preserved pore-like structures that could represent phloem-sieve areas (Figs 1f,h,k, S3j, S4e–h).

The endodermis is well-preserved in several axes and in transverse section consists of a single layer of mostly rectangular and polygonal cells with moderately thick walls (Figs 1f,i,k, S1c, S4d–h). Endodermal cells are *c.* 30–47 µm by *c.* 49–75 µm in transverse section, and up to *c.* 100–400 µm long. Pericycle primarily one-cell, occasionally two-cells wide, composed of elliptical to polygonal cells that are slightly thinner and smaller (*c.* 25–40 µm by *c.* 38–60 µm) than those of the surrounding endodermis (Figs 1f,i,k, S1c, S4d–h).

The cortex is *c.* 0.1–0.7 mm wide in transverse sections and contains consistently two ill-defined layers, an inner, dark brown, sclerenchymatous zone, and an outer, lighter brown, parenchymatous zone (Figs 1a,c–f, 2, S1, S3, S4d–h, S5). The thickness of the sclerenchymatous and parenchymatous zones is highly variable, with either cortex predominant or weakly developed. Cells of the sclerenchymatous cortex with thick, strongly lignified cells walls with slightly branched pits, and narrow and irregularly shaped lumen that are mostly elliptical to circular in outline and range from *c.* 15–45 µm in diameter, up to occasionally > 60 µm in diameter (Figs 1i,j, S4f,j,k). Cells of the parenchymatous cortex thin-walled, mostly circular in outline, ranging from *c.* 10–55 µm in diameter (Figs 1f,i, S4l). The epidermis is not preserved in most of the axes, but when present is composed of one to three layers of polygonal cells that are mostly rectangular in outline and *c.* 10–15 µm in diameter in

cross-section (Figs 1a, S1a,b, S3a). Neither aerenchyma nor corticular emergent roots are present in the cortex of any of the specimens.

Only the holotype shows attached well-developed microphylls (Figs 1a,b, 2, S1a, S2). All microphylls are of similar form (isophyllous) and none show evidence of a ligule. Three-dimensional reconstructions from micro-CT data show that the microphylls are *c.* 0.5–0.8 mm wide near the base, up to *c.* 1.5–2.0 mm long, dorsiventrally flattened proximally, with an acute apex, and entire margin (Fig. 2). Microphylls appear alternate, spirally arranged in six to eight ranks, and widely spaced between alternating subwhorls (Fig. 2; Video S1). In successive transverse sections microphylls are first seen as small bulges on the axis surface (Figs 1a, S1a, S2a,b). Separation occurs first along the lateral margins and continues for *c.* 0.1–0.3 mm, forming a slightly contracted, decurrent base (Figs 1a, 2). In transverse section, microphylls are more or less elliptical in outline as they separate from the axis, but become rhomboidal after full separation and then triangular near the apex (Figs 1a,b, 2, S2a–d).

Microphyll vasculature consists of a single, unbranched amphicribral vascular strand, *c.* 19–40 µm in diameter in transverse section, with elliptical to circular xylem (Figs 1b, 2b, S2a–e). Xylem is composed of radially aligned tracheids, *c.* 2–5 µm in diameter; phloem is not preserved. Surrounding the vascular strand is a well-defined parenchymatous layer without intercellular spaces that is composed of up to four rows of cells abaxially (*c.* 70–75 µm thick), and one to two rows of cells thick adaxially (*c.* 17–23 µm thick) (Figs 1b, S1a,b, S2). Individual parenchyma cells are *c.* 6–40 µm in diameter and are mostly circular to elliptical in outline, but rarely polygonal. An additional poorly-defined parenchymatous layer *c.* 16–25 µm thick is present adaxially. In this layer the individual cells and air spaces are usually crushed (Figs 1b, S2c,d). An epidermal layer one-cell thick is present on both the abaxial and adaxial surfaces of the microphyll (Fig. S2).
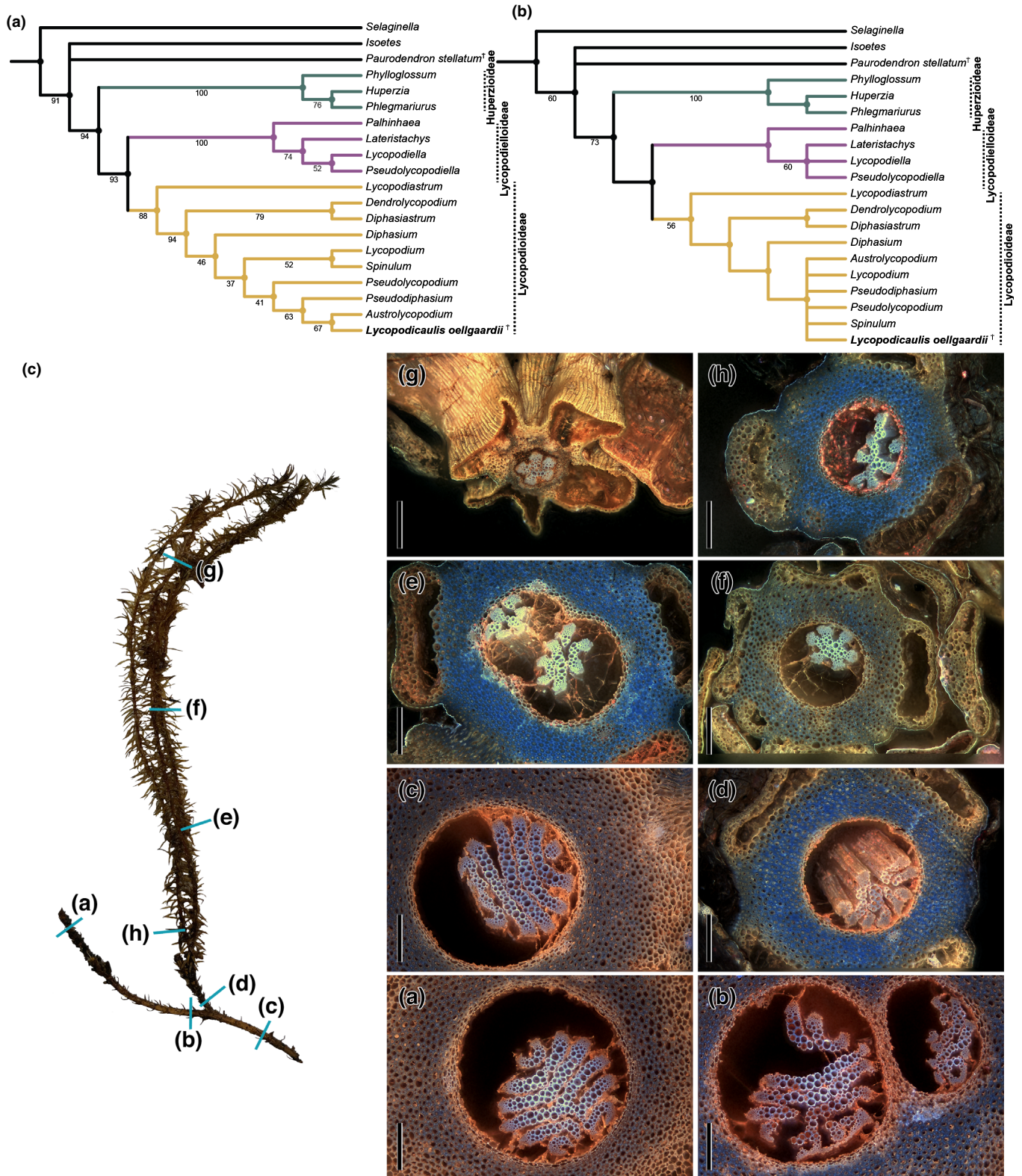
**Fig. 4** Phylogenetic relationships of Lycopodiaceae and *Lycopodicaulis oellgaardii* gen. et sp. nov. based on maximum likelihood (ML) (a) and maximum parsimony (MP) analyses (b). Both trees are rooted with *Isoetes* and *Selaginella*. (a) ML resolves *Lycopodicaulis* as sister to *Austrolycopodium* in crown Lycopodioideae. (b) MP, based on a strict consensus of 24 most parsimonious trees (length 1079 steps, consistency index (CI) 0.684, retention index (RI) 0.589, and rescaled consistency index (RC) 0.403) places *Lycopodicaulis* in a polychotomy within crown Lycopodioideae. Numbers below the lines are bootstrap values greater than 50%. (c) *Spinulum annotinum* (Lycopodioideae) under fluorescence microscopy (Lumen 200 Fluorescence Illumination System; filter set 02: G 365, FT 395, LP 420), (VT: Testo 2473, USA), serial transverse sections of a terrestrial lycopsid with creeping to erect axes showing variation in the dissection and shape of the protostele. Creeping axis showing thick sclerenchymatous inner cortex and actino–plectostele (sections a–c). Erect axes showing variation from actino–plectostele to actinostele, note microphylls with large air spaces (sections d–h). Bar, 200 µm.

Individual epidermal cells have anticlinal walls *c.* 8–11 µm long and *c.* 4–7 µm wide (Figs 1b, S2b–d,f). The cuticle is thin, *c.* 1.7–2.2 µm thick. No lacunae are evident on the microphylls and stomata or trichomes have not been observed (Fig. S2f).

Leaf traces are present in the stelar region and cortex of several axes that lack well-developed microphylls (Figs 1k, S3j, S4c,h,i, S5). Leaf traces are found connected to protoxylem poles in the stele (e.g. Fig. 1k), departed from the stele and located near its periphery (Fig. S4h), and within the middle of the cortex of the axes (Figs S3j, S5). In all cases, the leaf trace, as it leaves the vascular cylinder, is very small, but rapidly increases in size in the cortex. In the stele, leaf traces are *c.* 19–25 µm in diameter and composed of a few tracheids, whereas in the cortex leaf traces are *c.* 36–40 µm in diameter and consist of one or two rows of tracheids. Cortical leaf traces show a distinctive parenchymatous bundle sheath, consisting of polygonal cells, *c.* 8–15 µm in diameter (Figs S3j, S4h,i, S5h).

## Phylogenetic systematics

The topologies of our ML and MP trees are concordant except for a lack of resolution within core subfamily Lycopodioideae in the MP tree (Fig. 4a,b). Both analyses recover three principal clades within Lycopodiaceae, corresponding to the three widely recognized subfamilies Huperzioideae, Lycopodioideae, and Lycopodielloideae (PPG I, 2016) with strong support; however, support for internal nodes is generally low. In both phylogenies, *Lycopodicaulis oellgaardii* is resolved within subfamily Lycopodioideae; it is sister to *Austrolycopodium* in the ML tree (Fig. 4a) and placed in a polytomy with five extant genera in the MP tree (Fig. 4b).

## Discussion

### Comparison of *Lycopodicaulis* with extant Lycopodiales

*Lycopodicaulis oellgaardii* is assigned to the Lycopodiaceae (Lycopodiopsida) based mainly on the anisotomous, unbranched or dichotomously branched axes with an actinostelic, actino–plectostelic to plectostelic protostele, combined with microphylls that lack a ligule and are supplied by a vascular strand that does not produce a leaf gap (Figs 1, 2, S1–S5). The absence of rhizophores at branch points (i.e. *Selaginella*) and the apparent lack of rhizomorphous roots (i.e. *Isoetes*) are also consistent with a relationship to Lycopodiaceae.

Within Lycopodiaceae, extant genera in subfamily Huperzioideae (i.e. *Huperzia*, *Phlegmariurus*, and *Phylloglossum*) differ from *Lycopodicaulis oellgaardii* in that the protostele occupies less than one-third of the total stem diameter, the cortex is primarily composed of parenchyma, occasionally with aerenchyma, and the presence of corticular emergent roots (Figs 3r–x, S8). Axes of *Lycopodicaulis oellgaardii* also differ from those of genera of subfamily Lycopodielloideae (i.e. *Lateristachys*, *Lycopodiella*, *Palhinhaea*, and *Pseudolycopodiella*) because the cortex in this subfamily is predominantly parenchymatous, and in many species of *Lycopodiella* and *Pseudolycopodiella* it also

contains prominent aerenchyma (Figs 3n–q, S9–S11). In some species of *Palhinhaea* (Figs 3q, S10) (see also Rowe *et al.*, 2004), it is also the inner cortex that is parenchymatous while the outer cortex is sclerenchymatous; the reverse of the condition in the fossil axes (Figs 1a,c–f, S1, S3–S5).

The leafy axes of *Lycopodicaulis oellgaardii* are most similar to those of plants in subfamily Lycopodioideae (i.e. *Austrolycopodium*, *Dendrolycopodium*, *Diphasiastrum*, *Diphasium*, *Lycopodiastrum*, *Lycopodium*, *Pseudodiphasium*, *Pseudolycopodium*, and *Spinulum*). All species of Lycopodioideae for which we have examined anatomy consistently have a protostele that occupies more than one-third of the total stem diameter, as in the fossil material, as well as inner sclerenchymatous and outer parenchymatous zones in the cortex (Figs 3a–m, 4c, S6, S7). Variations in the form of the protostele in the fossils (Figs 1a,c,d, 2e–g, S3, S5) are also consistent with the natural variation observed along the axes of extant species of the subfamily (Figs 4c, S6, S7). As also are changes in protostele dissection before and after dichotomous branching, which are similar to those seen in living species of *Lycopodium* (Gola *et al.*, 2007) that have also been interpreted as anatomical and physiological adaptations of the vascular system for terrestrial conditions (see Gola *et al.*, 2007, and references cited therein).

Microphylls of *Lycopodicaulis oellgaardii* also resemble those of many Lycopodioideae, and especially *Austrolycopodium*, *Dendrolycopodium*, *Lycopodium*, and *Spinulum* in which all microphylls are of the same size and shape (isophyllous), spirally arranged (3–8 ranks), and dorsiventrally flattened proximally. Microphylls of extant species of *Lycopodium* differ in the presence of hair-like hyaline apices.

Taken together, the anatomical and morphological features of both the axes and microphylls support the placement of *Lycopodicaulis oellgaardii* from the Lower Cretaceous of Inner Mongolia in crown group Lycopodiaceae, and specifically within Lycopodioideae. This assignment suggests that if the strobili of *Lycopodicaulis* are eventually recovered that in addition to being homosporous they should have deciduous subpeltate to peltate sporophylls.

### Comparison of *Lycopodicaulis* with other fossil Lycopodiales

A variety of fossils from the Mesozoic of Eurasia have been attributed to lycopsids (e.g. Krassilov, 1967; Na *et al.*, 2017; Volynets & Bugdaeva, 2017; Frolov & Mashchuk, 2019) but most have been assigned to *Lycopodites*. Except for *Lycopodites hannahensis* Harris (Harris, 1976; Thomas, 2017), all are preserved as compressions or impressions, and hence are difficult to compare with *Lycopodicaulis oellgaardii* from Inner Mongolia. Potentially most relevant are the dichotomous axes of Early Cretaceous age from China, *Lycopodites ovatus* Deng from the fine-grained sandstones/siltstones of the Huolinhe Formation in Huolinhe Basin (Deng, 1995), and *Lycopodites multifurcatus* Li, Ye et Zhou from the Jiaohe Basin (Li *et al.*, 1987). Nevertheless, both taxa differ from *Lycopodicaulis oellgaardii*. *Lycopodites ovatus* is based on compression fossils and while its anisotomously

branched axes are similar to *Lycopodicaulis* in size, its leaves are anisophyllous and arranged in two ranks. *Lycopodites multifurcatus* Li, Ye et Zhou is isophyllous, but the microphylls are in two ranks and flat.

*Lycopodites hannahensis* first described from Lower Cretaceous of southern England (Harris, 1976) and later from the Middle Jurassic of Yorkshire (Thomas, 2017) is known from isophyllous, dichotomizing vegetative axes and has been suggested to be an erect marsh plant (Harris, 1976; Thomas, 2017). The axes are poorly preserved, but in the material from the Middle Jurassic of Yorkshire there is a partially pyritized exarch protostele comparable to that of extant lycopsids. Other details of the stele, cortex, and microphylls are not preserved.

Silicified axes of a possible lycopodiaceous affinity are known from the Lower Cretaceous (initially reported as Jurassic) of India (Srivastava, 1946; Mittre, 1958; Surange, 1966; Banerji, 2000) and have been referred to the fossil genus *Lycoxylon* (Srivastava) Mittre. Axes of *Lycoxylon* are small (up to *c.* 2 mm in diameter), likely herbaceous, and their exarch protosteles (more than one-third of total stem diameter) vary from plectostelic to actinostelic, with a thin sclerified cortex. The Indian axes are somewhat similar to those of living Lycopodioideae; however, whether a ligule is present or definitively absent remains unknown, and no microphylls or leaf traces are preserved. The thin structure of the cortex and the near V-shaped arrangement of the stele are also very different from that of *Lycopodicaulis*. Detailed reexamination of the *Lycoxylon* material is necessary to secure a tentative assignment to the Lycopodioideae.

*Collinsonites* Schwendemann, Decombeix, Taylor et Taylor from the Late Permian of Antarctica is known from compressions and impressions of herbaceous, dichotomizing stems that bear spirally arranged eligulate microphylls (Schwendemann *et al.*, 2010) that are associated with permineralized sporophylls attributed to *Collinsonostrobus* Ryberg, Taylor et Taylor (Ryberg *et al.*, 2012) that may be part of the same species (McLoughlin *et al.*, 2015). The anatomy of *Collinsonites* is unknown, but differs from *Lycopodicaulis* in the presence of conspicuous spinose margins of some of the microphylls.

Against this background of previously described homosporous lycopsids, the excellent preservation of *Lycopodicaulis oellgaardii* is matched only by the quality of preservation seen in the putative lycopsid *A. mackiei* from the Rhynie Chert (Kidston & Lang, 1920, 1921; Kerp *et al.*, 2013; Hetherington *et al.*, 2021) from which *A. mackiei* differs in the absence of true microphylls, the presence of a strongly lacunate cortex, and a predominantly and poorly dissected actinostele. The well characterized anatomical and morphological features of *Lycopodicaulis oellgaardii* distinguish it from all other taxa in the extensive fossil record of the lycopsids and provide support for recognizing a new genus placed unequivocally in crown Lycopodiaceae that is most closely related to extant Lycopodioideae.

## Implications for the evolution of crown clubmosses

Extant Lycopodioideae are mainly terrestrial, unlike many species of the Huperzioideae (Øllgaard, 1995, 2015; Field *et al.*, 2016), including, for example, *Phylloglossum*, which grows in habitats that are very wet seasonally (Fig. 3x), the many primarily tropical species of *Phlegmariurus*, which are mainly epiphytes (Fig. 3r–u), and the bog clubmoss *Lycopodiella* in Lycopodielloideae (Figs 3o, p, S9, S10). These ecological differences are reflected in the anatomy of the stems of the three subfamilies (Figs 3, 4c, S6–S11). The terrestrial, often erect stems, as well as their rhizomes, in Lycopodioideae are composed of a stout protostele with an inner sclerenchymatous cortex. In contrast, in Huperzioideae and Lycopodielloideae, the protostele is relatively small, and the cortex is predominantly parenchymatous/aerenchymatous. These observations suggest that *Lycopodicaulis* was an upright plant of terrestrial habitats. It was preserved not as whole plants, but as fragments swept into an allochthonous peat along with other plant debris, including fragments of wood, roots, ferns, corystosperm cupules and cones and leaves of conifers (see Matsunaga *et al.*, 2021; G. Shi *et al.*, 2021).

The anatomical and morphological similarities of fossil *Lycopodicaulis oellgaardii* to extant Lycopodioideae (Figs 1–3, 4c) provide the basis for its inclusion in phylogenetic analyses of living and fossil lycopsids in a combined morphological and DNA sequence dataset (Fig. 4a,b). Analyses using both parsimony and ML recover the three subfamilies recognized by previous hypotheses of relationships among extant Lycopodiaceae (Field *et al.*, 2016; Bauret *et al.*, 2018; Testo *et al.*, 2018a). A strict consensus tree of the 24 most parsimonious trees resulting from analysis using parsimony places *Lycopodicaulis oellgaardii* in a polytomy with extant *Austrolycopodium*, *Lycopodium*, *Pseudodiphasium*, *Pseudolycopodium*, and *Spinulum* (Fig. 4b). Analysis using ML gave improved resolution (Fig. 4a) placing *Lycopodicaulis oellgaardii* as sister to *Austrolycopodium* in crown Lycopodioideae, with both nested well within the group including the other extant genera of subfamily Lycopodioideae.

Placement of *Lycopodicaulis oellgaardii* in crown Lycopodiaceae is consistent with the relatively young age of the fossils compared to the long evolutionary history of the family, including the early presence of *Asteroxylon*, but provides a key secure data point from which to calibrate molecular clock analyses of divergence times within the family. Previous estimates of the age of crown Lycopodiaceae spanned > 200 Myr and ranged from the Jurassic to the Devonian, *c.* 167 to *c.* 369 Ma (e.g. Wikström & Kenrick, 2001; Laenen *et al.*, 2014; Larsén & Rydin, 2016; Testo *et al.*, 2018a). Secure placement of *Lycopodicaulis oellgaardii* within crown Lycopodioideae establishes that this clade was already present in Asia by the Early Cretaceous in Asia (late Barremian–earliest Aptian, $125.6 \pm 1.0$ Ma) and is consistent with hypotheses that suggest divergences within the subfamily likely occurred during the Jurassic, perhaps in association with the initial breakup of Pangaea (Testo *et al.*, 2018a).

## Author contributions

GS, FH, PSH and PRC discovered the new Early Cretaceous permineralized peat and collected the paleobotanical samples. FH and GS prepared the fossil material; FH and EGC processed the micro-CT data; FH and WLT collected herbarium and living plant material; FH obtained living anatomical data and images; FH, WLT and ARF provided the morphological matrix; FH and WLT carried out phylogenetic analyses; FH wrote the manuscript in discussion with WLT, ARF, EGC, PSH, PRC and GS.

## ORCID

Elizabeth G. Clark https://orcid.org/0000-0003-4289-6370
Peter R. Crane https://orcid.org/0000-0003-4331-6948
Ashley R. Field https://orcid.org/0000-0002-0139-7914
Patrick S. Herendeen https://orcid.org/0000-0003-2657-8671
Fabiany Herrera https://orcid.org/0000-0002-2412-672X
Gongle Shi https://orcid.org/0000-0003-3374-6637
Weston L. Testo https://orcid.org/0000-0003-3194-5763

## Data availability

The data that support the findings of this study are openly available in Figshare at doi: 10.6084/m9.figshare.14925369 and MorphoBank at http://morphobank.org/permalink/?P3664.

## References

**Arana MD, Reinoso H, Oggero AJ. 2014.** Morfología y anatomía de ejes caulinares, licofilos y esporangios de *Phlegmariurus phylicifolius*: un aporte a la sistemática de las Lycopodiaceae Neotropicales. *Revista de Biologia Tropical* **62**: 1217–1227.

**Ayensu ES. 1967.** Aerosol OT solution—an effective softener of herbarium specimens for anatomical study. *Biotechnic & Histochemistry* **42**: 155–156.

**Banerji J. 2000.** Megafloral diversity of the upper Gondwana sequence of the Rajmahal Basin, India. *Journal of African Earth Sciences* **31**: 133–144.

**Bateman RM, Kenrick P, Rothwell GW. 2007.** Do eligulate herbaceous lycopsids occur in Carboniferous strata? *Hestia eremosa* gen. et sp. nov. from the Mississippian of Oxroad bay, east Lothian, Scotland. *Review of Palaeobotany and Palynology* **144**: 323–335.

**Bauret L, Field AR, Gaudeul M, Selosse M-A, Rouhan G. 2018.** First insights on the biogeographical history of *Phlegmariurus* (Lycopodiaceae), with a focus on Madagascar. *Molecular Phylogenetics and Evolution* **127**: 488–501.

**Bruce JG. 1976.** Development and distribution of mucilage canals in *Lycopodium*. *American Fern Journal* **63**: 481–491.

**Carlquist S, Schneider EL, Kenneally KF. 2012.** SEM studies on tracheids of Lycopodiaceae; observations on adaptations in *Phylloglossum*. *American Fern Journal* **102**: 273–282.

**Chu MCY. 1974.** A comparative study of the foliar anatomy of *Lycopodium* species. *American Journal of Botany* **61**: 681–692.

**Cignoni P, Callieri M, Corsini M, Dellepiane M, Ganovelli F, Ranzuglia G. 2008.** MESHLAB: an open-source mesh processing tool. In: *Sixth Eurographics Italian chapter conference*. Salerno, Italy, 129–136.

**Cleal C, Thomas B. 2019.** Lycophytes. In: *Introduction to plant fossils, 2nd edn.* Cambridge, UK: Cambridge University Press, 73–98.

**Deng S. 1995.** *Early Cretaceous Flora of Huolinhe Basin, Inner Mongolia, Northeast China*. Beijing, China: Geological Publishing House.

**Elpe C, Knopf P, Stützel T, Schulz C. 2018.** Diversity and evolution of leaf anatomical characters in Taxaceae s.l.—fluorescence microscopy reveals new delimitating characters. *Journal of Plant Research* **131**: 125–141.

**Field AR, Testo W, Bostock PD, Holtum JAM, Waycott M. 2016.** Molecular phylogenetics and the morphology of the Lycopodiaceae subfamily Huperzioideae supports three genera: *Huperzia*, *Phlegmariurus* and *Phylloglossum*. *Molecular Phylogenetics and Evolution* **94**: 635–657.

**Frolov AO, Mashchuk IM. 2019.** Taxonomy of the Genus *Lycopodites* (Lycopodiales) from the Jurassic Sediments of the Irkutsk Basin (East Siberia). *The Bulletin of Irkutsk State University. Series Biology. Ecology* **28**: 3–16.

**Galtier JM, Phillips TL. 1999.** The acetate peel technique. In: Jones TP, Rowe NP, eds. *Fossil plants and spores: modern techniques*. London, UK: Geological Society of London, 67–70.

**Gola EM, Jernstedt JA, Zagórska-Marek B. 2007.** Vascular architecture in shoots of early divergent vascular plants, *Lycopodium clavatum* and *Lycopodium annotinum*. *New Phytologist* **174**: 774–786.

**Harris TM. 1976.** A slender upright plant from Wealden sandstones. *Proceedings of the Geologists' Association* **87**: 413–422.

**Hetherington AJ, Bridson SL, Jones AL, Hass H, Kerp H, Dolan L. 2021.** An evidence-based 3D reconstruction of *Asteroxylon mackiei*, the most complex plant preserved from the Rhynie chert. *eLife* **10**: e69447.

**Hill JB. 1914.** The anatomy of six epiphytic species of *Lycopodium*. *Botanical Gazette* **58**: 61–85.

**Jones CE. 1905.** The morphology and anatomy of the stem of the genus *Lycopodium*. *Transactions of the Linnean Society of London* **27**: 15–36.

**Joy KW, Willis AJ, Lacey WS. 1956.** A rapid cellulose peel technique in palaeobotany. *Annals of Botany* **20**: 635–637.

**Kazhdan M, Hoppe H. 2013.** Screened Poisson surface reconstruction. *ACM Transactions on Graphics* **32**: 1–13.

**Kenrick P, Crane PR. 1997.** *The origin and early diversification of land plants a cladistic study*. Washington, DC, USA: Smithsonian Books.

**Kerp H, Wellman CH, Krings M, Kearney P, Hass H. 2013.** Reproductive organs and in situ spores of *Asteroxylon mackiei* Kidston & Lang, the most complex plant from the Lower Devonian Rhynie Chert. *International Journal of Plant Sciences* **174**: 293–308.

**Kidston R, Lang WH. 1920.** On Old Red Sandstone plants showing structure, from the Rhynie Chert Bed, Aberdeenshire. Part III. *Asteroxylon mackiei*, Kidston and Lang. *Transactions of the Royal Society of Edinburgh Earth Science* **52**: 643–680.

**Kidston R, Lang WH. 1921.** On Old Red Sandstone plants showing structure, from the Rhynie Chert Bed, Aberdeenshire. Part IV. Restorations of the vascular cryptogams, and discussion of their bearing on the general morphology of the Pteridophyta and the origin of the organisation of land plants. *Transactions of the Royal Society of Edinburgh Earth Science* **52**: 831–854.

**Krassilov VA. 1967.** *Lower Cretaceous Flora of Southern Primor'e and its importance for stratigraphy*. Moscow, Russia: Akademii Nauk SSSR [in Russian].

**Laenen B, Shaw B, Schneider H, Goffinet B, Paradis E, Désamoré A, Heinrichs J, Villarreal JC, Gradstein SR, McDaniel SF et al. 2014.** Extant diversity of

bryophytes emerged from successive post-Mesozoic diversification bursts. *Nature Communications* **5**: 1–6.

**Larsén E, Rydin C. 2016.** Disentangling the phylogeny of *Isoetes* (Isoetales), using nuclear and plastid data. *International Journal of Plant Sciences* **177**: 157–174.

**Li X, Ye M, Zhou Z. 1987.** Late Early Cretaceous flora from Shansong, Jiaohe, Jilin Province, northeast China. *Palaeontologia Cathayana* **3**: 1–53.

**Lopes LKC, Góes-Neto LAA, Feio AC. 2020.** Stem anatomy and its relevance for the taxonomic survey of *Selaginella* subg. Gymnogynum (Selaginellaceae). *Plant Systematics and Evolution* **306**: 13.

**Matsunaga KK, Herendeen PS, Herrera F, Ichinnorov N, Crane PR, Shi G. 2021.** Ovulate cones of *Schizolepidopsis ediae* sp. nov. provide insights into the evolution of Pinaceae. *International Journal of Plant Sciences* **182**: 490–507.

**McLoughlin S, Drinnan AN, Slater BJ, Hilton J. 2015.** *Paurodendron stellatum*: a new Permian permineralized herbaceous lycopsid from the Prince Charles Mountains, Antarctica. *Review of Palaeobotany and Palynology* **220**: 1–5.

**Mittre V. 1958.** Studies on the fossil flora of Nipania, Rajmahal series, India – Pteridophyta, and general observations on Nipania fossil flora. *The Palaeobotanist* **7**: 47–66.

**Na Y, Sun C, Wang H, Dilcher DL, Li Y, Li T. 2017.** A brief introduction to the Middle Jurassic Daohugou Flora from Inner Mongolia, China. *Review of Palaeobotany and Palynology* **247**: 53–67.

**Øllgaard B. 1975.** Studies in the Lycopodiaceae I. Observations of the structure of the sporangium wall. *American Fern Journal* **65**: 19–27.

**Øllgaard B. 1979.** Studies in Lycopodiaceae, II. The branching patterns and infrageneric groups of *Lycopodium* sensu lato. *American Fern Journal* **69**: 49–61.

**Øllgaard B. 1987.** A revised classification of the Lycopodiaceae s. lat. *Opera Botanica* **92**: 153–178.

**Øllgaard B. 1992.** Neotropical lycopodiaceae-an overview. *Annals of the Missouri Botanical Garden* **79**: 687–717.

**Øllgaard B. 1995.** Diversity of *Huperzia* (Lycopodiaceae) in neotropical montane forests. In: Churchill SP, Balslev H, Forero E, Luteyn JE, eds. *Biodiversity and conservation of Neotropical montane forests*. New York, NY, USA: The New York Botanical Garden Press, 349–358.

**Øllgaard B. 2015.** Six new species and some nomenclatural changes in neotropical Lycopodiaceae. *Nordic Journal of Botany* **33**: 186–196.

**Pixley EY. 1968.** A study of the ontogeny of the primary xylem in the roots of *Lycopodium*. *Botanical Gazette* **129**: 156–160.

**PPG I. 2016.** A community-derived classification for extant lycophytes and ferns. *Journal of Systematics and Evolution* **54**: 563–603.

**Rincón-Baron EJ, Hilda-Rolleri C, Alzate-Guarin F, Dorado-Gálvez JM. 2014.** Ontogenia de los esporangios, formación y citoquímica de esporas en licopodios (Lycopodiaceae) colombianos. *Revista de Biología Tropical* **62**: 273–298.

**Rowe N, Isnard S, Speck T. 2004.** Diversity of mechanical architectures in climbing plants: an evolutionary perspective. *Journal of Plant Growth Regulation* **23**: 108–128.

**Ryberg PE, Taylor EL, Taylor TN. 2012.** Permineralized lycopsid from the Permian of Antarctica. *Review of Palaeobotany and Palynology* **169**: 1–6.

**Schwendemann AB, Decombeix AL, Taylor EL, Taylor TN. 2010.** *Collinsonites schopfii* gen. et sp. nov., a herbaceous lycopsid from the Upper Permian of Antarctica. *Review of Palaeobotany and Palynology* **158**: 291–297.

**Shi G, Herrera F, Herendeen PS, Clark EG, Crane PR. 2021.** Mesozoic cupules and the origin of the angiosperm second integument. *Nature* **594**: 223–226.

**Shi GL, Li JG, Tan T, Dong C, Li QL, Wu Q, Zhang BL, Yin SX, Herrera F, Herendeen PS** *et al.* **2021.** Age of the Huolinhe Formation in the Huolinhe Basin, eastern Inner Mongolia, China: evidence from U-Pb zircon dating and palynological assemblages. *Journal of Stratigraphy* **45**: 69–81.

**Skog JE, Hill CR. 1992.** The Mesozoic herbaceous lycopsids. *Annals of the Missouri Botanical Garden* **79**: 648–675.

**Spencer V, Nemec Venza Z, Harrison CJ. 2021.** What can lycophytes teach us about plant evolution and development? Modern perspectives on an ancient lineage. *Evolution & Development* **23**: 174–196.

**Srivastava BP. 1946.** Silicified plant remains from the Rajmahal series of India. *Proceedings of the National Academy of Sciences India* **15**: 185–211.

**Stevenson DW. 1976.** Observations on phyllotaxis, stelar morphology, the shoot apex and gemmae of *Lycopodium lucidulum* Michaux (Lycopodiaceae). *Botanical Journal of the Linnean Society* **72**: 81–100.

**Stokey AG. 1907.** The roots of *Lycopodium pithyoides*. *Botanical Gazette* **44**: 57–63.

**Surange KR. 1966.** Indian fossil Pteridophytes. *Botanical Monograph* **4**: 1–195.

**Swofford DL. 2003.** *PAUP\*: phylogenetic analysis using parsimony (\* and other methods), v.4.* Sunderland, MA, USA: Sinauer.

**Taylor TN, Taylor EL, Krings M. 2009.** *Paleobotany: the biology and evolution of fossil plants, 2nd edn.* Burlington, VT, USA: Academic Press.

**Testo WL, Field AR, Barrington DS. 2018a.** Overcoming among-lineage rate heterogeneity to infer the divergence times and biogeography of the clubmoss family Lycopodiaceae. *Journal of Biogeography* **45**: 1929–1941.

**Testo WL, Øllgaard B, Field AR, Almeida T, Kessler M, Barrington DS. 2018b.** Phylogenetic systematics, morphological evolution, and natural groups in Neotropical *Phlegmariurus* (Lycopodiaceae). *Molecular Phylogenetics and Evolution* **125**: 1–13.

**Thomas BA. 1992.** Palaeozoic herbaceous lycopsids and the beginnings of extant *Lycopodium* sens. lat. and *Selaginella* sens. lat. *Annals of the Missouri Botanical Garden* **79**: 623–631.

**Thomas BA. 1997.** Upper Carboniferous herbaceous lycopsids. *Review of Palaeobotany and Palynology* **95**: 129–153.

**Thomas BA. 2017.** The occurrence of *Lycopodites hannahensis* Harris in the Yorkshire Jurassic together with details of its anatomy. *Proceedings of the Yorkshire Geological Society* **61**: 281–283.

**Trifinopoulos J, Nguyen L-T, von Haeseler A, Minh BQ. 2016.** W-IQ-Tree: a fast online phylogenetic tool for maximum likelihood analysis. *Nucleic Acids Research* **44**: W232–W235.

**Volynets E, Bugdaeva E. 2017.** The Aptian-Cenomanian flora of the Razdolnaya coal Basin (Primorye region, Russia). *Island Arc* **26**: e12171.

**Warmbrodt RD, Evert RF. 1974a.** Structure and development of the sieve element in the stem of *Lycopodium lucidulum*. *American Journal of Botany* **61**: 267–277.

**Warmbrodt RD, Evert RF. 1974b.** Structure of the vascular parenchyma in the stem of *Lycopodium lucidulum*. *American Journal of Botany* **61**: 437–443.

**Wikström N, Kenrick P. 2001.** Evolution of Lycopodiaceae (Lycopsida): estimating divergence times from *rbcL* gene sequences by use of nonparametric rate smoothing. *Molecular Phylogenetics and Evolution* **19**: 177–186.

**Wilder GJ. 1970.** Structure of tracheids in three species of *Lycopodium*. *American Journal of Botany* **57**: 1093–1107.

## Supporting Information

Additional Supporting Information may be found online in the Supporting Information section at the end of the article.

**Fig. S1** *Lycopodicaulis oellgaardii* gen. et sp. nov.

**Fig. S2** *Lycopodicaulis oellgaardii* gen. et sp. nov.

**Fig. S3** *Lycopodicaulis oellgaardii* gen. et sp. nov.

**Fig. S4** *Lycopodicaulis oellgaardii* gen. et sp. nov.

**Fig. S5** *Lycopodicaulis oellgaardii* gen. et sp. nov.

**Fig. S6** *Dendrolycopodium obscurum.*

**Fig. S7** *Diphasiastrum digitatum.*

**Fig. S8** *Huperzia lucidula.*

**Fig. S9** *Lycopodiella inundata.*

**Fig. S10** *Lycopodiella prostrata.*

**Fig. S11** *Palhinhaea cernua.*

**Table S1** Specimen information of living Lycopodiaceae anatomically analyzed in this study.

**Table S2** List of morphological characters/states and matrix for phylogenetic analyses.

**Table S3** GenBank accession numbers for the DNA sequence data used in the phylogenetic analyses.

**Video S1** Reconstructed slice data for holotype showing transverse sections of axis and microphylls.

Please note: Wiley Blackwell are not responsible for the content or functionality of any Supporting Information supplied by the authors. Any queries (other than missing material) should be directed to the *New Phytologist* Central Office.